

# A Near-Vertical Slab Tear in the Southeastern Solomon Islands

Ching-Yu Cheng<sup>1</sup>, Hao Kuo-Chen<sup>2</sup>, Wei-Fang Sun<sup>3</sup>, Chin-Shang Ku<sup>4</sup>, Yu-Ting Kuo<sup>5</sup>, Bor-Shouh Huang<sup>6</sup>, and Yue-Gau Chen<sup>7</sup>

<sup>1</sup>National Central University

<sup>2</sup>National Taiwan University

<sup>3</sup>National Dong Hwa University

<sup>4</sup>Academia Sinica

<sup>5</sup>National Chung Cheng University

<sup>6</sup>Institute of Earth Sciences, Academia Sinica, Taiwan

<sup>7</sup>Research Center for Environmental Changes, Academia Sinica

June 1, 2023

## Abstract

The Solomon Islands is one of the most seismically active areas in the southern Pacific with high earthquake hazard potential. The regional seismic network, equipped with six broadband seismic stations, was constructed as late as October 2018. On January 27 and 29, 2020, two moderate earthquakes, Mw 6.3 and 6.0, respectively, occurred in the southeastern Solomon Islands. The entire foreshock-main-shock-aftershock sequence was recorded by this seismic network for exploring the seismogenic structures. Based on the spacial distribution of the foreshock-aftershock sequence, the interaction of the subduction and transform zones between the Pacific and the Australia plates could lead to the near-vertical dip-slip tear slab. Confirmed with PREM and the new 1D velocity model for testing the robustness of the earthquake locations, a seismic gap at depths from 25 to 35 km is observed as the “jelly sandwich” rheology of the continental crust of the Australia plate.

# A Near-Vertical Slab Tear in the Southeastern Solomon Islands

C.-Y. Cheng<sup>1</sup>, H. Kuo-Chen<sup>2\*</sup>, W.F. Sun<sup>2</sup>, C.-S. Ku<sup>3</sup>, Y.-T. Kuo<sup>4</sup>, B.-S. Huang<sup>3</sup>, and Y.-G. Chen<sup>5</sup>

<sup>1</sup>Department of Earth Sciences, National Central University.

<sup>2</sup>Department of Geosciences, National Taiwan University.

<sup>3</sup>Institute of Earth Sciences, Academia Sinica.

<sup>4</sup>Department of Earth and Environmental Sciences, National Chung Cheng University.

<sup>5</sup>Research Center for Environmental Changes, Academia Sinica.

Corresponding author: Hao Kuo-Chen ([kuochenhao@ntu.edu.tw](mailto:kuochenhao@ntu.edu.tw))

## Key Points:

- An optimized local 1D velocity model was determined from the regional seismic network.
- A subduction-to-strike-slip transition system could result in the near-vertical dip-slip tear slab in the southeastern Solomon Islands.
- The “jelly sandwich” rheology of the continental crust of the Australia Plate is observed.

## 21 **Abstract**

22 The Solomon Islands is one of the most seismically active areas in the southern Pacific with  
23 high earthquake hazard potential. The regional seismic network, equipped with six broadband  
24 seismic stations, was constructed as late as October 2018. On January 27 and 29, 2020, two  
25 moderate earthquakes, Mw 6.3 and 6.0, respectively, occurred in the southeastern Solomon  
26 Islands. The entire foreshock-main-shock-aftershock sequence was recorded by this seismic  
27 network for exploring the seismogenic structures. Based on the spacial distribution of the  
28 foreshock-aftershock sequence, the interaction of the subduction and transform zones between the  
29 Pacific and the Australia plates could lead to the near-vertical dip-slip tear slab. Confirmed with  
30 PREM and the new 1D velocity model for testing the robustness of the earthquake locations, a  
31 seismic gap at depths from 25 to 35 km is observed as the “jelly sandwich” rheology of the  
32 continental crust of the Australia plate.

33

## 34 **Plain Language Summary**

35 To establish a seismic network is always the first step and essential for studying any  
36 researches related to earthquakes, especially in the Solomon Islands, one of the most seismically  
37 active areas in the southern Pacific. However, as late as October 2018, the regional seismic network  
38 in the southeastern Solomon Islands, equipped with six broadband seismic stations, was  
39 constructed because most of the areas are inaccessible. A good 1D local velocity model is crucial  
40 for determining earthquake locations. The data set from foreshock-main-shock-aftershock  
41 sequence of two earthquakes in 2020 recorded in the seismic network provides a good opportunity  
42 for obtaining a 1D velocity model. After the reliable earthquake locations are determined, the  
43 spacial distribution of the foreshock-aftershock sequence can provide valuable information about  
44 seismogenic structures for better understanding the occurrence of earthquakes. As a result, a near-  
45 vertical dip-slip slab of the Australia plate from the subsurface to 120 km with a seismic gap at  
46 depths from 25 to 35 km is observed for the first time. This near-vertical tear slab could result from  
47 a subduction-to-strike-slip transition system and the seismic gap within the continental crust is  
48 related to “jelly sandwich” rheology.

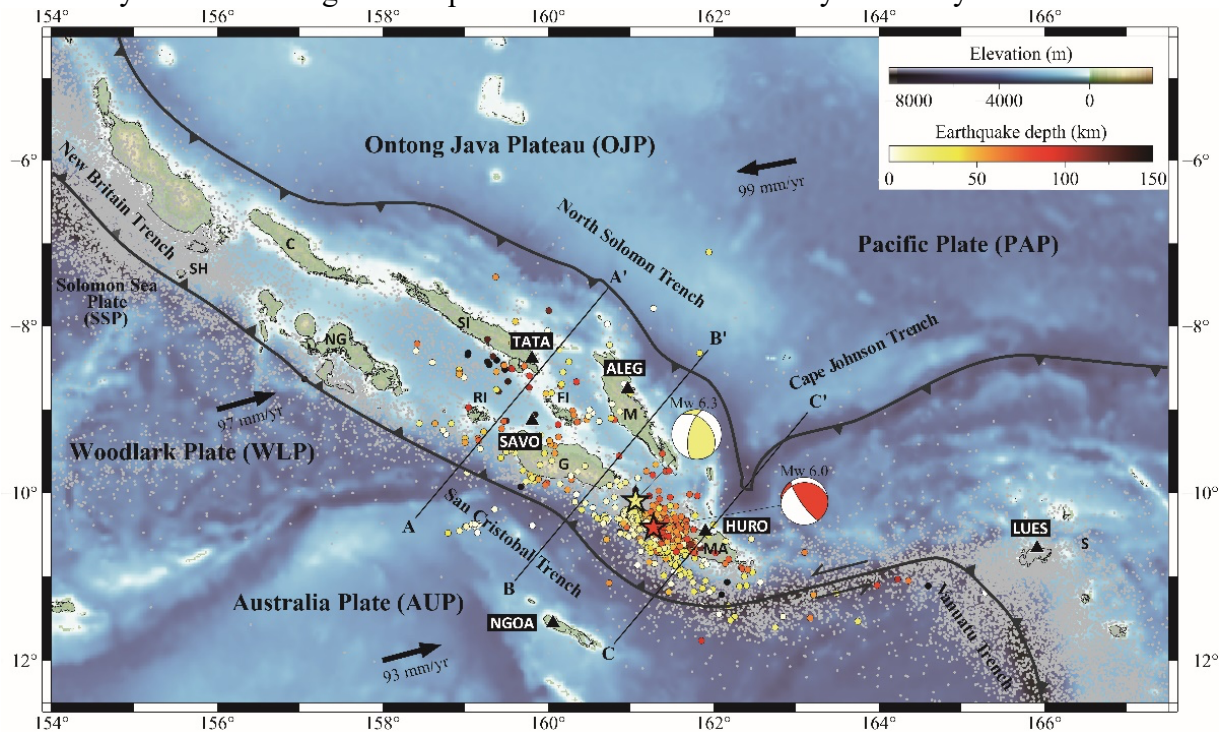
49

## 50 **1 Introduction**

51 Previous studies in the Solomon Islands have mainly focused on tectonic evolution (e.g., Yan  
52 and Kroenke, 1993; Mann et al., 1998; Petterson et al., 1999; Mann and Taira, 2004; Holm et al.,  
53 2016), geology (e.g., Mann et al., 1998; Taylor et al., 2005; Taylor et al., 2008; Chen et al., 2011),  
54 and a few related to the crustal and upper mantle structures using ocean-bottom seismometer data  
55 set with passive and active sources (e.g., Mann et al., 1996; Phinney et al., 1999; Mann and Taira,  
56 2004; Miura et al., 2004). The subduction systems in the southeastern Solomon Islands have not  
57 been documented in detail due to shortages of seismic stations and feasible data for investigating  
58 the complex seismogenic, crustal, and upper mantle structures. The complex tectonic setting and  
59 geopolitical marginality make the Solomon Islands hardly to be explored, including deploying  
60 seismic stations on islets. However, improvement of station coverage, in particular, is one of the  
61 most effective observations to answer the seismotectonic debate (e.g., Ku et al., 2020).

62 The regional seismic monitoring network in the southeastern Solomon Islands was  
63 constructed until October 2018 (Fig. 1). On January 27 and 29, 2020, two moderate

64 earthquakes, Mw 6.3 and Mw 6.0, respectively, occurred in the southeastern Solomon Islands. The  
 65 entire foreshock-main-shock-aftershock sequences were completely recorded by this regional-  
 66 scale seismic network. These two earthquakes are located in the most active area of the region,  
 67 which the foreshock and aftershock sequences can provide a unique opportunity to look into the  
 68 crustal and upper mantle structures of the subduction zones between the Pacific plate (PAP) and  
 69 the Australia plate (AUP). Here, we report on earthquake distribution for the southeastern  
 70 termination of the southeastern Solomon Islands subduction zone and also derive a optimized local  
 71 1D velocity model utilizing the complete seismic data recorded by the newly seismic network.



72  
 73 **Figure 1.** Topography, bathymetry, and regional tectonic setting of the Solomon Islands region.  
 74 Arrows indicate direction and rate of plate motion of the Australia, Pacific, and Woodlark plates  
 75 (NUVEL-1A, Demets et al., 1994); heavy lines with triangles represent subduction boundaries;  
 76 black triangles are broadband seismic stations; yellow and orange stars represent earthquakes  
 77 occurred on January 27 and 29 from the Incorporated Research Institutions for Seismology (IRIS)  
 78 catalog; focal mechanisms of the two earthquakes are from GCMT; circles color-coded by depth  
 79 indicate foreshocks and aftershocks recorded by GNS seismic stations; background seismicity are  
 80 shown as gray dots and are compiled by the IRIS event catalog for the period 1971-2021; AA',  
 81 BB' and CC' are the cross sections in Figs. 2-5. SH, Shortland Islands; C, Choiseul; NG, New  
 82 Georgia Island Group; SI, Santa Isabel; RI, Russell Islands; FI, Florida Islands; G, Guadalcanal;  
 83 M, Malaita; MA, Makira; SCZ, Santa Cruz Islands.

## 85 2 Tectonic setting

86 The Solomon Islands is located in a complex and active plate boundary where several  
 87 plates interact with each other, including the PAP, the AUP, and the associated microplates (i.e.,  
 88 the Woodlark plate (WLP) and Solomon Sea plate (SSP)) (Fig. 1) (e.g., Demets et al., 1990, 1994,  
 89 2010; Beavan et al., 2002; Miura et al., 2004; Phinney et al., 2004; Taira et al., 2004; Taylor et al.,  
 90 2005, 2008; Argus et al., 2011; Newman et al., 2011). In the southern Solomon Islands, the WLP  
 91 and the AUP subduct beneath the PAP forming the New Britain Trench, San Cristobal Trench and

92 Vanuatu Trench (e.g., Taylor and Exon, 1987; Crook and Taylor, 1994; Taylor et al., 1995; Mann  
93 et al., 1998; Taylor et al., 2005). The area surrounding the Solomon Islands and the Santa Cruz  
94 Islands contains two subduction-to-strike-slip transition (SSST) regions where a transform zone  
95 links two oblique subduction zones (Bilich et al., 2001). In addition, the Ontong Java Plateau of  
96 the PAP, the largest and thickest oceanic plateau on Earth, subducts along the North Solomon  
97 Trench and the Cape Johnson Trench in the north with slight convergence (e.g., Taylor and Exon,  
98 1987; Yan and Kroenke, 1993; Crook and Taylor, 1994; Mann et al., 1998; Petterson et al., 1999;  
99 Mann and Taira, 2004). The Solomon arc is assumed the most representative example of an island  
100 arc polarity reversal due to the presence of inwardly double subduction zones resulting in high risk  
101 of earthquakes, tsunamis, and volcanic eruptions.

102 Composed of two chains of islands, the Solomon Islands extends about 1000 km wide  
103 which are partitioned into multiple segments by distinct geological or seismological characteristics  
104 (e.g., Mann et al., 1998; Taylor et al., 2005; Chen et al., 2011). Nowadays, the active subduction  
105 occurs in the southeast of the Solomon Islands along the San Cristobal Trench according to  
106 previous seismological investigations from global seismic networks (e.g., Cooper and Taylor,  
107 1987; Mann et al., 1998; Chen et al., 2011). They found that it might be caused by strongly oblique  
108 subduction occurring southeast of the region, although the structures of subduction zones is still  
109 under debate.

110

### 111 **3 Seismic network and data processing**

112 The Institute of Geological and Nuclear Sciences Limited (GNS), New Zealand, deployed six  
113 permanent seismic stations in different islets of the southeastern Solomon Islands since October  
114 2018 (Fig. 1). The instruments are equipped with broadband seismometer (Trillium 120PA;  
115 Nanometrics Inc., Canada) and 24-bits digital recorder (Q330S; Quanterra Inc., U.S.A.) with  
116 sampling rates of 100 Hz. Except for the timing problem of the station LUES, most of the seismic  
117 waveforms recorded by the other five stations have good signal-to-noise ratios. To date, this  
118 seismic network is maintained by the Ministry of Mines, Energy and Rural Electrification of the  
119 Solomon Islands Government.

120 In this study, we processed two-month continuous seismic waveforms from this seismic  
121 network, one month before and after the two main shocks, respectively, to well cover the period  
122 of the whole earthquake sequence. The data set is formatted with the daily miniSEED and we used  
123 the SeisAn Earthquake analysis software (SEISAN) to establish the event database (Havskov and  
124 Ottemoller, 1999). Most of the events occurred close to the seismic network so that we were able  
125 to extract numerous high-quality seismic waveforms to pick P- and S-wave arrivals, locate  
126 earthquakes and determine magnitudes. We located earthquakes by the HYPOCENTER program  
127 (e.g., Lienert et al., 1986) and determined moment magnitude ( $M_w$ ) by spectral analysis. More  
128 details of the waveform analysis procedure are described in Havskov and Ottemoller (2010).

129 The earthquake catalog contains events detected by at least three stations and has more than  
130 one clear S-wave arrival to effectively constrain the depths of earthquakes. The interpolated 1D  
131 Preliminary Reference Earth Model (PREM) (Dziewonski and Anderson, 1981) was used as the  
132 reference model. In total, 730 earthquakes were listed in the preliminary catalog and of which 651  
133 were located within the seismic network. We used the program VELEST (Kissling, 1988, Kissling  
134 et al., 1994) to derive a 1D velocity model, which produces the smallest possible uniform error for  
135 a set of seismic events with well-constrained locations. We select events within the range of the  
136 seismic network with the root-mean-square error in arrival time from 0.5 to 1.0 s to invert a new

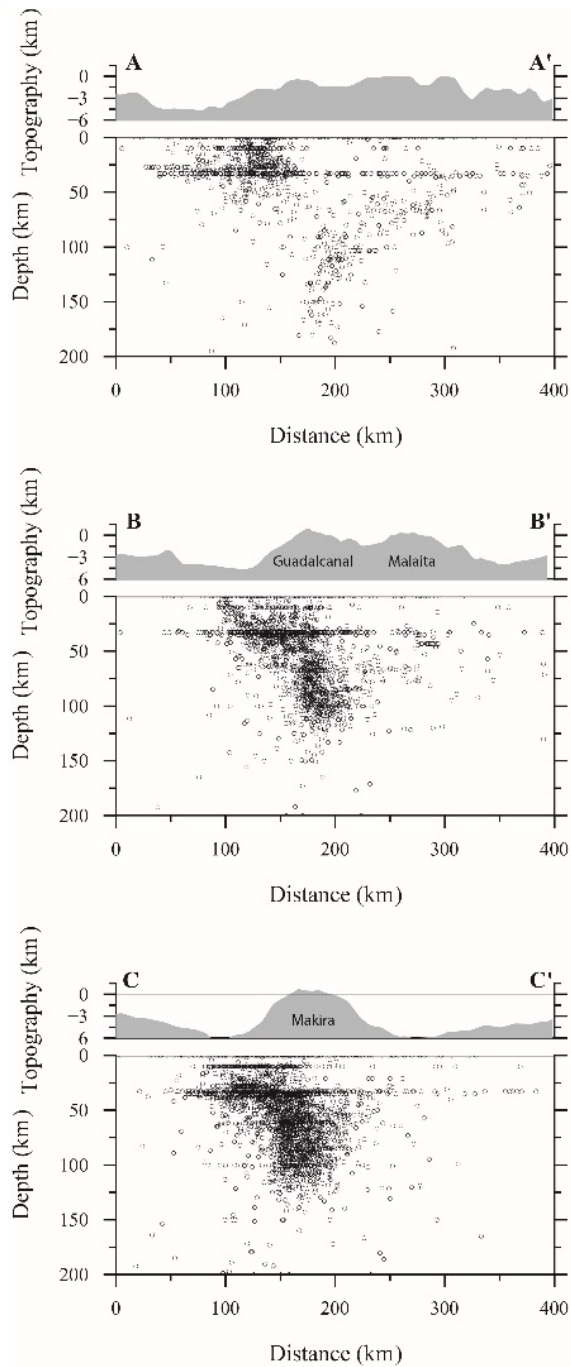
137 1D velocity model. In total, 389 events were selected for inversion to derive the preferred 1D  
138 model and then with it we relocated all 730 earthquakes to obtain the final catalog.

139

#### 140 **4 Results**

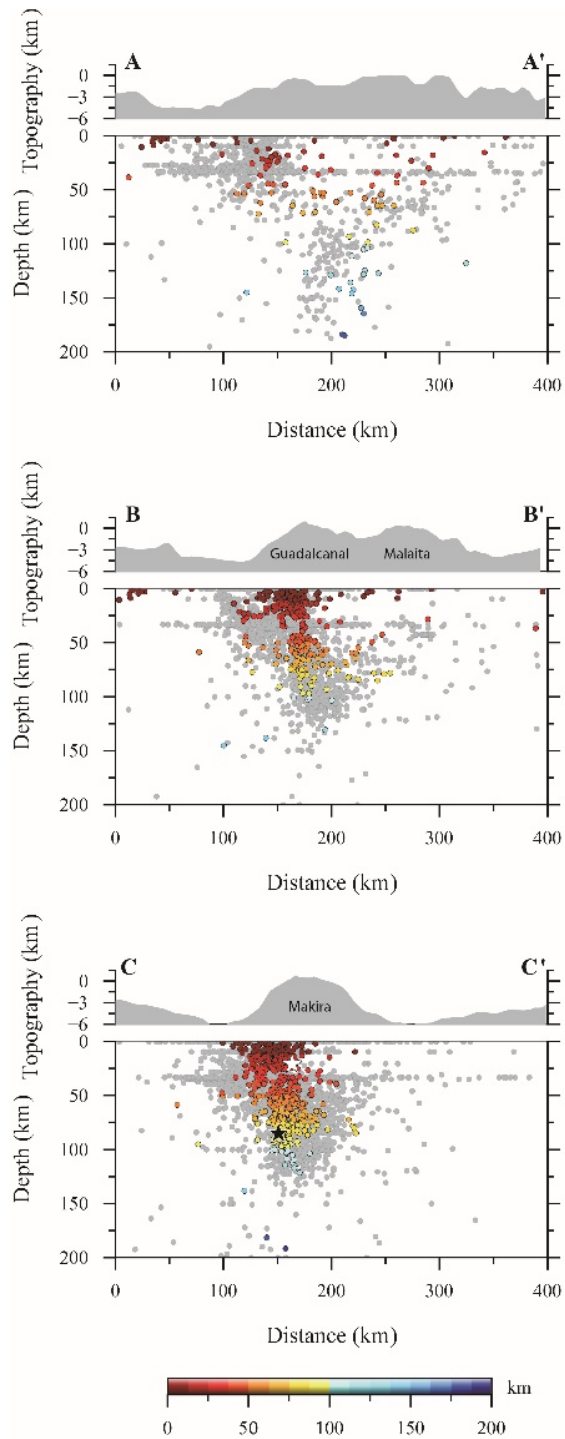
141 The background seismicity is extracted from the global earthquake catalog from 1971-2021  
142 compiled by the Incorporated Research Institutions for Seismology (IRIS) (Fig. 2). In 50 years,  
143 only ~5100 events in our study area are listed in the IRIS catalog because of poor constraints of  
144 station coverage. The hypocenters of the two main shocks, reported by IRIS, distribute apart from  
145 depths at 21 and 85 km, respectively (cross-section CC' of Fig. 3). During the same time period,  
146 January and February 2020, only 23 earthquakes are listed in the IRIS catalog but 730 are detected  
147 from our new data set. Obviously, we detected a significant number of missing events, especially  
148 at shallow depths that also appear with steep dip, the same as the deeper events (cross-sections  
149 BB' and CC' of Fig. 3). Relatively, in contrast, our results at deep depth show a similarity of high  
150 dip angle with background seismicity but are more concentrated at the San Cristobal Trench (cross-  
151 sections BB' and CC' of Fig. 3).

152 Among the 730 events, the standard error of the means in vertical location (ERZ), in  
153 horizontal location (ERH), and root-mean-square error in arrival time of event locations are  $24.7$   
154  $\pm 19.15$  km,  $13.43 \pm 10.8$  km, and  $0.61 \pm 0.30$  s, respectively. The moment magnitudes ( $M_w$ )  
155 determined in this study mostly range from 2.0 to 4.0. The main earthquake cluster is located  
156 between Makira and Guadalcanal (Fig. 1), one of the most active regions in the Solomon Islands,  
157 where commonly experiences large earthquakes (Chen et al., 2011). Events in the cluster extend  
158 from subsurface to 120 km depth which is similar to the previous studies (Cooper and Taylor,  
159 1985; Mann and Taira, 2004). Three southwest-northeast cross sections nearly perpendicular to  
160 the subduction zone show spatial variation of foreshocks and aftershocks from northwest to  
161 southeast (Figs. 2 and 3). Two southeastern cross sections close to the main shocks reveal that the  
162 event cluster is near-vertical and can be divided into shallow ( $< 25$  km) and deep (35-120 km)  
163 parts (cross-sections BB' and CC' of Fig. 3). Although the North Solomon Trench contains fewer  
164 earthquakes, the cross sections in the northwest do show two trenches subduct inwardly (cross-  
165 sections AA' and BB' of Fig. 3). Fig. 4 presents the cross sections of the relocated earthquakes  
166 with the new 1D velocity model. Both the location results with PREM and the new 1D velocity  
167 model reveal a steep event cluster, but the new velocity model has low-velocity zone at 10 km  
168 depth and slower velocity layer within depths of 25-35 km comparing with PREM (Fig. 5).



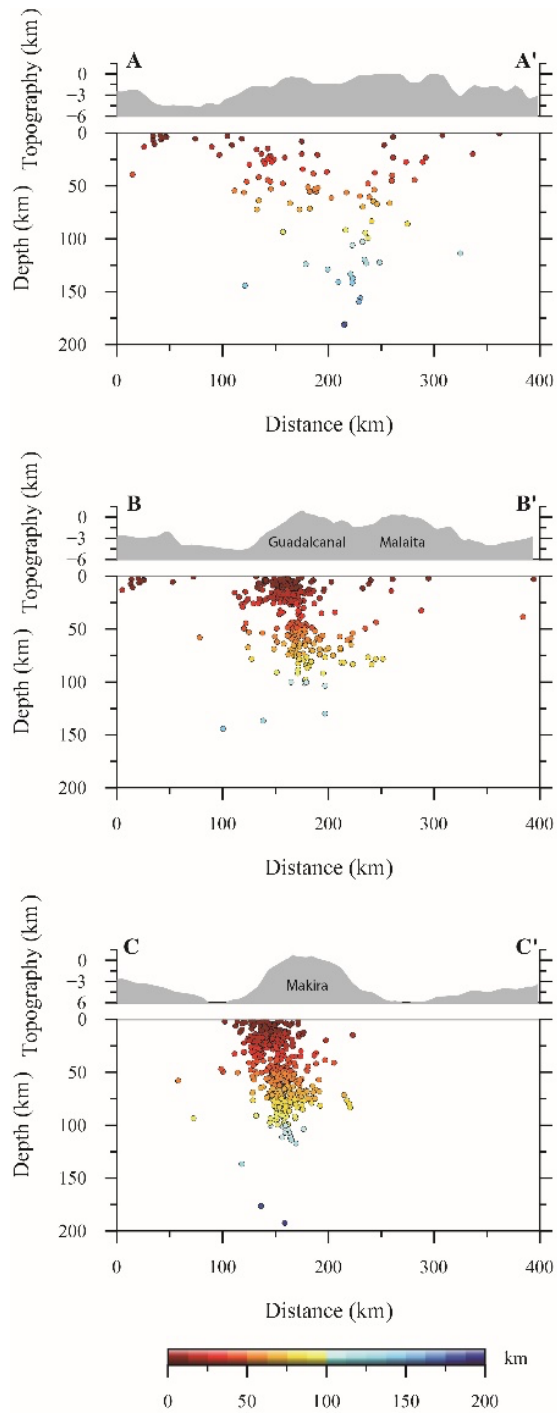
169  
170  
171  
172  
173

**Figure 2.** Cross sections of background seismicity around the southeastern Solomon Islands are compiled by IRIS event catalog from the period 1971-2021. Earthquake hypocenters are projected onto the three 200-km-wide transects shown in Fig. 1. Topography of three area is projected on to profiles in the upper panels.



174  
175  
176  
177  
178  
179

**Figure 3.** Comparison of earthquake hypocenters in this study and background seismicity. Cross sections with background seismicity (gray dots) and foreshocks and aftershocks (circles color-coded by depth); project lines are shown in Fig. 1; background seismicity is the same as Fig. 2; white and black stars represent January 27 and 29 earthquakes from IRIS event catalog.

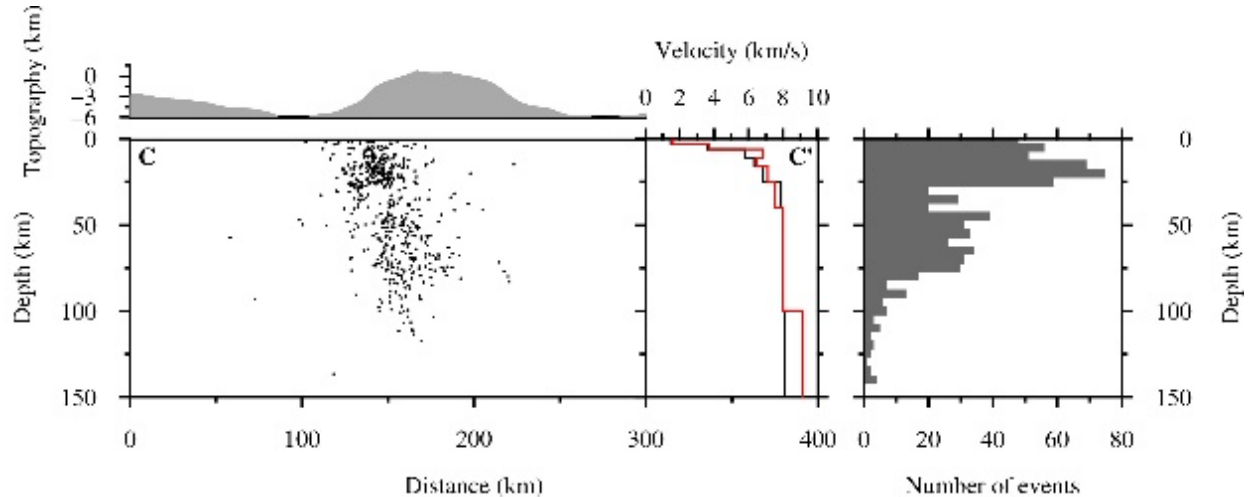


180

181

182

**Figure 4.** Cross sections of earthquake hypocenters relocated by the new 1D velocity model. Circles color-coded by depth are foreshocks and aftershocks; project lines are shown in Fig. 1.



183  
 184 **Figure 5.** CC' cross section (in Fig. 4) with the seismic cluster relocated by the new velocity model  
 185 around the southeastern Solomon Islands. The middle panel shows the 1D interpolated PREM  
 186 (black line) and the new velocity model (red line); the right panel is the event distribution in 5 km  
 187 depth intervals. Note the seismic gap between 25 km and 35 km depths.

188

## 189 5 Discussions

190 The Solomon arc, expanding ~1000 km wide, is characterized by diverse fault geometry as  
 191 well as subduction properties in different segments. The complexity of tectonic setting in the  
 192 Solomon Islands also makes the behavior of the seismic activities vary along the island chain. With  
 193 background seismicity from the 1971-2021 IRIS catalog in the Solomon Islands, majority of the  
 194 earthquakes occurred along the San Cristobal Trench which is much more seismically and  
 195 volcanically active than that of the early developed subduction zones to the north (Fig. 1). These  
 196 earthquakes, moreover, mainly distributed between Makira and Guadalcanal, show different  
 197 structural states from the northwestern side to the southeastern through the hypocenter transects  
 198 (Figs. 2 and 3). Many studies used seismicity from different global catalogs and time periods to  
 199 propose the subduction manifestation, including the dip angle and the depth of the two slabs from  
 200 the San Cristobal Trench and the North Solomon Trench (Cooper and Taylor, 1985; Mann and  
 201 Taira, 2004; Miura et al., 2004). Cooper and Taylor (1985) and Mann and Taira (2004) gave  
 202 different points of view from a similar distribution of seismicity between Makira and Guadalcanal  
 203 that the latter slab angle was much flatter than the former one. However, we have different  
 204 perspective of the subduction structure beneath the southeastern Solomon Islands from previous  
 205 studies due to the better quality constrains on the new seismic data set.

206 Based on our results, we suggest that the event cluster does show as a steep seismogenic  
 207 structure in the corner zone within the SSST between the Solomon Islands and the Santa Cruz  
 208 Islands and also could interpret it as the location of near-vertical dip-slip tear within the Australia  
 209 lithosphere (Fig. 5). This complicated plate configuration as a SSST region, which has been found  
 210 at least 30 locations on Earth (Bilich et al., 2001), is usually with damaged earthquakes occurred  
 211 frequently. The seismicity concentrates at the edge of the tear which extends almost vertically from  
 212 the subsurface to ~120 km. Govers and Wortel (2005) assumed that the intersection between the  
 213 subduction and the transform propagates through the lithosphere, inducing a tearing transform  
 214 fragment. They refer to the tearing as a subduction-transform edge propagator (STEP) fault and  
 215 developed the STEP model to interpret vertical, dip-slip tearing at perpendicular plate boundaries,

216 for example, the northern Tonga (Isacks et al., 1969; Millen and Hamburger, 1998) and the  
217 southeast corner of the Caribbean (Molnar and Sykes, 1969; Clark et al., 2008). According to  
218 Bilich et al. (2001), the southeastern Solomon Islands is one of the SSST regions where the  
219 northeastward subduction of the AUP connects the transition of northeast-southwest transform  
220 motion between the PAP and the AUP. We believe that the vertical motions and complex  
221 deformation revealed by the seismicity can demonstrate the tear propagation right beneath Makira  
222 and Guadalcanal. The suggestion is also consistent with Bilich et al. (2001) that the southeastern  
223 Solomon corner zone features a band of mechanisms which nearly reach the strike-slip corner (Fig.  
224 6).

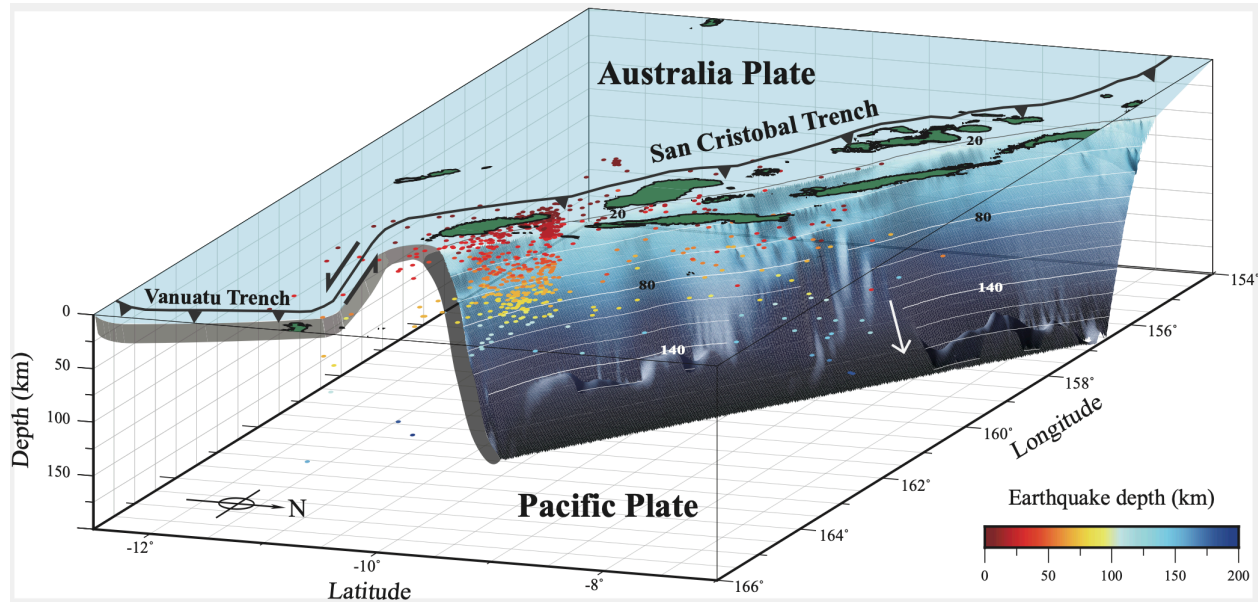
225 We also observe a seismic gap, both located by PREM (Fig. 3) and the new velocity model  
226 (Fig. 4), which is similar to the seismic cluster in the Lesser Antilles of the South American plate  
227 and this phenomenon is suggested that the gap is a weak, ductile, lower crustal layer separating a  
228 strong upper/middle crustal layer from a strong lithospheric layer (Clark et al., 2008). The seismic  
229 gap, known as the “jelly sandwich” rheology (Chen and Molnar, 1983; Watts and Burov, 2003),  
230 detaches the subducting and the buoyant pieces of the AUP along a near-vertical tear here. In  
231 comparison to significant strength in the dry upper mantle, the weak lower crust would show as  
232 the undried granulite in the continental lithosphere (Jackson, 2002). The whole seismogenic  
233 deformation is about 100 km wide and extends 120 km through the entire crust and lithosphere  
234 and the gap is at 25-35 km depth within the tear.

235 In order to derive the local 1D velocity model for earthquake location procedures, we use the  
236 program VELEST to construct the new velocity model in the southeastern Solomon Islands. In  
237 comparison with the interpolated PREM, the seismicity relocated by the new velocity model  
238 reveals that the earthquakes at shallow depth (~10 km) become deeper and the cluster also becomes  
239 more concentrated. Besides, a new optimized velocity model has a low-velocity layer around 10  
240 km depth and slower velocity from 20-35 km depth. Ku et al. (2020) also observed a low-velocity  
241 zone above the Moho in the Western Solomon Islands and they referred it to the lower crustal  
242 magma (Dufek and Bergantz, 2005). The distribution of the root-mean-square error in arrival times  
243 are more centralized after relocating and that may indicate the new optimized velocity model is  
244 more appropriate for this region. However, the cross sections in Fig. 4 show the appearance of  
245 earthquakes that relocated with the new velocity model is similar to Fig. 3, which events are located  
246 with the interpolated PREM. We can observe the seismic gap at depths of 20-35 km in both results  
247 which confirms the authenticity of the seismogenic structure.

248 Comparing the result with background seismicity, not only do we locate more earthquakes at  
249 shallow depth, but we also locate events more concentrated than the prior catalog (Fig. 3). We  
250 assume that nearby stations and the interpolated 1D PREM or the new velocity model constrain  
251 the quality of the result so that we can locate lots of earthquakes with small magnitude and at  
252 shallow depth. Owing to the complete seismic data recorded by the newly seismic network, we  
253 interpret the event cluster beneath Makira and Guadalcanal to define the location of active tearing  
254 within the Australia lithosphere, at the corner zone between the San Cristobal Trench and  
255 transform zone (Fig. 6).

256

257



258  
 259 **Figure 6.** Three-dimensional visualization of the seismic cluster in the southeastern Solomon  
 260 Islands viewed from northwest. Heavy lines with barbs represent subduction boundaries; solid  
 261 contour lines are Slab2 – A Comprehensive Subduction Zone Geometry Model (Hayes et al.,  
 262 2018), contoured every 20 km; earthquake hypocenters (circles) show crustal and mantle  
 263 seismicity gathers at 100 km-wide seismic cluster, at the edge of the lithospheric tear.

264

## 265 6 Conclusions

266 In this study, we provide better quality constraints on locating earthquakes with a new  
 267 optimized local 1D velocity model from the regional seismic network and discover the  
 268 seismogenic mechanisms and structures in the southeastern Solomon Islands. The earthquake  
 269 cluster between Makira and Guadalcanal distributes near vertically from subsurface to 120 km  
 270 depth, which is interpreted as the tear slab within the Australia lithosphere, due to the interaction  
 271 of subduction and transform zones of the PAP and AUP. A seismic gap observed at depths of 25-  
 272 35 km sustains a “jelly sandwich” rheology of the continental crust.

273

## 274 Acknowledgments

275 This project is supported by Academic Sinica (Grant NO. AS-TP-110-M02). The  
 276 assistance from Mr. Douglas Billy and Mr. Carlos Tatapu of Geological Survey Division, Solomon  
 277 Islands Ministry of Mines, Energy and Rural Electrification (MMERE) are highly appreciated.

278

## 279 Open Research

280 The seismic data set used in this manuscript is available on  
 281 <https://tecdc.earth.sinica.edu.tw/WAV/2020SolomonIs/> (login with Email:  
 282 solomon@earth.sinica.edu.tw and password: Islands2023).  
 283 Maps were created by using Generic Mapping Tools (GMT) version 6 (Wessel et al., 2019).

284

285

286 **References**

- 287 Argus, D. F., R. G. Gordon, and C. DeMets (2011). Geologically current motion of 56 plates  
288 relative to the no-net-rotation reference frame, *Geochemistry, Geophysics, Geosystems* **12**, no.  
289 11.
- 290 Beavan, J. P., M. Tregoning, M. Bevis, and C. Meertens (2002). Motion and rigidity of the Pacific  
291 plate and implications for plate boundary deformation, *J. Geophys. Res.* **107**, 2261.
- 292 Bilich A., C. Frohlich, and P. Mann (2001). Global seismicity characteristics of subduction-to-  
293 strike-slip transitions, *J. Geophys. Res.* **106**, no. B9, 19433-19452.
- 294 Chen M. C., C. Frohlich, F. W. Taylor, G. Burr, and A. Q. van Ufford (2011). Arc segmentation  
295 and seismicity in the Solomon Islands arc, SW Pacific, *Tectonophysics* **507**, 47-69.
- 296 Chen, W. P., and P. Molnar (1983). Focal depths of intracontinental and intraplate earthquakes  
297 and their implications of the thermal and mechanical properties of the lithosphere, *J. Geophys.*  
298 *Res.* **88**, no. B5, 4183-4214.
- 299 Clark, S. A., M. Sobiesiak, C. A. Zelt, M. B. Magnani, M. S. Miller, M. J. Bezada, and A. Levander  
300 (2008). Identification and tectonic implications of a tear in the South American plate at the  
301 southern end of the Lesser Antilles, *Geochemistry, Geophysics, Geosystems* **9**, no. 11.
- 302 Cooper, P. A., and B. Taylor (1985). Polarity reversal in the Solomon Islands arc, *Nature* **314**,  
303 428-430.
- 304 Cooper, P. A., and B. Taylor (1987). Seismotectonics of New Guinea: a model for arc reversal  
305 following arc-continent collision, *Tectonics* **6**, 53-67.
- 306 Crook, K., and B. Taylor, (1994). Structure and Quaternary tectonic history of the Woodlark triple  
307 junction region, Solomon Islands, *Marine Geophysical Researches* **16**, 65-89.
- 308 DeMets, C., R. G. Gordon, and D. F. Argus (2010). Geological current plate motions, *Geophys. J.*  
309 *Int.* **181**, 1-80.
- 310 DeMets, C., R. G. Gordon, D. F. Argus, and S. Stein (1990). Current plate motions, *Geophys. J.*  
311 *Int.* **101**, 425-478.
- 312 DeMets, C., R. G. Gordon, D. F. Argus, and S. Stein (1994). Effect of recent revisions to the  
313 geomagnetic reversal time scale on estimates of current plate motions, *Geophys. Res. Lett.* **21**,  
314 2191-2194.
- 315 Dufek, J., and G. W. Bergantz (2005). Lower crustal magma genesis and preservation: a stochastic  
316 framework for the evaluation of basalt-crust interaction. *J. Petrol.* **46**, 2167-2195.
- 317 Dziewonski, A. M., and D. L. Anderson (1981). Preliminary reference Earth model, *Physics of the*  
318 *Earth and Planetary Interiors* **25**(4), 297-356.
- 319 Forsyth, D. W. (1975). Fault plane solutions and tectonics of the South Atlantic and Scotia Sea, *J.*  
320 *Geophys. Res.* **80**, no. 11, 1429-1443.
- 321 Govers, R., and M. J. R. Wortell (2005). Lithosphere tearing at STEP faults: Response to edges  
322 of subduction zones, *Earth Planet. Sci. Lett.* **236**, 505-523.
- 323 Havskov, J., and L. Ottemoller (1999). SeisAn earthquake analysis software, *Seismol. Res. Lett.*  
324 **70**, no. 5, 532-534.
- 325 Havskov, J., and L. Ottemoller (2010). *Routine Data Processing in Earthquake Seismology*,  
326 Springer, Dordrecht, The Netherlands.
- 327 Hayes, G. P., G. L. Moore, D. E. Portner, M. Hearne, H. Flamme, M. Furtney, and G. M. Smoczyk  
328 (2018). Slab2, a comprehensive subduction zone geometry model, *Science* **362**, 58-61.
- 329 Holm, R. J., G. Rosenbaum, S. W. Richards (2016). Post 8 Ma reconstruction of Papua New

- 330 Guinea and Solomon Islands: Microplate tectonics in a convergent plate boundary setting,  
331 *Earth-Science Reviews* **156**, 66-81.
- 332 Isacks, B., L. R. Sykes, and J. Oliver (1969). Focal mechanisms of deep and shallow earthquakes  
333 in Tonga-Kermadec region and tectonics of island arcs, *Geol. Soc. Am. Bull.* **80**(8), 1443-1470.
- 334 Jackson, J. A. (2002). Strength of the continental lithosphere: time to abandon the jelly sandwich?,  
335 *GSA today* **12**, 4-10.
- 336 Kissling, E. (1988). Geotomography with local earthquake data, *Reviews of Geophysics.* **26**, no.  
337 4,659-698.
- 338 Kissling, E., W. L. Ellsworth, D. Eberhart-Phillips, and U. Kradolfer (1994). Initial reference  
339 model in local earthquake tomography, *J. Geophys. Res.* **99**, 19635-19646.
- 340 Ku, C. S., Y. T. Kuo, B. S. Huang, Y. G. Chen, and Y. M. Wu (2020). Seismic velocity structure  
341 beneath the Western Solomon Islands from the joint inversion of receiver functions and  
342 surface-wave dispersion curves, *Journal of Asian Earth Science* **195**, 104378.
- 343 Lienert, B. R. E., E. Berg, and L. N. Frazer (1986). Hypocenter: An earthquake location method  
344 using centered, scaled and adaptively least squares, *Bull. Seismol. Soc. Am.* **76**, 771-783.
- 345 Mann, P., and A. Taira (2004). Global tectonic significance of the Solomon Islands and Ontong  
346 Java Plateau convergent zone, *Tectonophysics* **389**, 137-190.
- 347 Mann, P., F. W. Taylor, M. B. Lague, A. Quarles, and G. Burr (1998). Accelerating late Quaternary  
348 uplift of the New Georgia Islands Group (Solomon Island arc) in response to subduction of  
349 the recently active Woodlark spreading center and Coleman seamount, *Tectonophysics* **295**,  
350 259-306
- 351 Mann, P., M. Coffin, T. Shipley, S. Cowley, E. Phinney, A. Teagan, K. Suyehiro, N. Takahashi,  
352 E. Araki, M. Shinohara, S. Miura, and L. Tivuru (1996). Researchers investigate fate of  
353 oceanic plateaus at subduction zones, *EOS Transactions American Geophysical Union* **77**,  
354 282-283.
- 355 Millen, D. W., and M. W. Hamburger (1998). Seismological evidence for tearing of the Pacific  
356 plate at the termination of the Tonga subduction zone, *Geology* **26**, no. 7, 659-662.
- 357 Miura S., K. Suyehiro, M. Shinohara, N. Takahashi, E. Araki, and A. Taira (2004). Seismological  
358 structure and implications of collision between the Ontong Java Plateau and Solomon Island  
359 Arc from ocean bottom seismometer-airgun data, *Tectonophysics* **389**, 191-220.
- 360 Molnar, P., and L. R. Sykes (1969). Tectonics of the Caribbean and Middle America region from  
361 focal mechanisms and seismicity, *Geol. Soc. Amer. Bull.* **80**, 1639.
- 362 Newman, A. V., L. J. Feng, H. M. Fritz, Z. M. Lifton, N. Kalligeris, and Y. Wei (2011). The  
363 energetic 2010  $M_w$  7.1 Solomon Islands tsunami earthquake, *Geophys. J. Int.* **186**, 775-781.
- 364 Petterson, M., T. Babbs, C. Neal, J. Mahoney, A. Saunders, R. Duncan, D. Tolia, R. Magu, C.  
365 Qopoto, H. Mahoa, and D. Natogga (1999). Geological-tectonic framework of Solomon  
366 Islands, SW Pacific: crustal accretion and growth within an intra-oceanic setting,  
367 *Tectonophysics* **301**, 35-60.
- 368 Phinney, E., P. Mann, M. Coffin, and T. Shipley (1999). Sequence stratigraphy, structure, and  
369 tectonics of the southwestern Ontong Java Plateau adjacent to the North Solomon trench and  
370 Solomon Islands arc, *J. Geophys. Res.* **104**, 20449-20466.
- 371 Phinney, E., P. Mann, M. Coffin, and T. Shipley (2004). Sequence stratigraphy, structural style,  
372 and age of deformation of the Malaita accretionary prism (Solomon arc-Ontong Java Plateau  
373 convergent zone), *Tectonophysics* **389**, 221-246.
- 374 Taira, A., P. Mann, and R. Rahardiawan (2004). Incipient subduction of the Ontong Java Plateau  
375 along the North Solomon trench, *Tectonophysics* **389**, 247-266.

- 376 Taylor, B., A. Goodliffe, F. Martinez, and R. Hey (1995). Continental rifting and initial sea-floor  
377 spreading in the Woodlark basin, *Nature* **374**, 534-537.
- 378 Taylor, B., and N. Exon (1987). An investigation of ridge subduction in the Woodlark – Solomons  
379 region: introduction and overview, in *Geology and Offshore Resources of the Pacific Island*  
380 *Arcs – Solomon Islands and Bougainville, Papua New Guinea regions* Taylor, B. (Editor),  
381 Circum-Pacific Council for Energy and Mineral Resources, vol. 7. Earth Science Series,  
382 Houston, TX, 1-24.
- 383 Taylor, F. W., P. Mann, M. G. Bevis, R. L. Edwards, H. Cheng, K. B. Cutler, S. C. Gray, G. S.  
384 Burr, J. W. Beck, D. A. Phillips, G. Cabioch, and J. Recy (2005). Rapid forearc uplift and  
385 subsidence caused by impinging bathymetric features: Examples from the New Hebrides and  
386 Solomon arcs, *Tectonics* **24**(6).
- 387 Taylor, F. W., R. W. Briggs, C. Frohlich, A. Brown, M. Hornbach, A. K. Papabatu, A. J. Meltzner,  
388 and D. Billy (2008). Rupture across arc segment and plate boundaries in the 1 April 2007  
389 Solomons earthquake, *Nature Geoscience* **1**, 253-257.
- 390 Watts, A. B., and E. B. Burov (2003). Lithospheric strength and its relationship to the elastic and  
391 seismogenic layer thickness, *Earth Planet. Sci. Lett.* **213**(1-2), 113-131.
- 392 Wessel, P., Luis, J. F., Uieda, L., Scharroo, R., Wobbe, F., Smith, W. H. F., & Tian, D. (2019).  
393 The Generic Mapping Tools version 6. *Geochemistry, Geophysics, Geosystems*, **20**, 5556–  
394 5564. <https://doi.org/10.1029/2019GC008515>.
- 395 Yan, C., and L. Kroenke (1993). A plate tectonic reconstruction of the SW Pacific, 0-100 Ma, in  
396 *Proceedings of the Ocean Drilling Program* Berger, T., Kroenke, L., Mayer, L., et al. (Editor),  
397 *Scientific Results* **130**, 697-709.
- 398
- 399

# A Near-Vertical Slab Tear in the Southeastern Solomon Islands

C.-Y. Cheng<sup>1</sup>, H. Kuo-Chen<sup>2\*</sup>, W.F. Sun<sup>2</sup>, C.-S. Ku<sup>3</sup>, Y.-T. Kuo<sup>4</sup>, B.-S. Huang<sup>3</sup>, and Y.-G. Chen<sup>5</sup>

<sup>1</sup>Department of Earth Sciences, National Central University.

<sup>2</sup>Department of Geosciences, National Taiwan University.

<sup>3</sup>Institute of Earth Sciences, Academia Sinica.

<sup>4</sup>Department of Earth and Environmental Sciences, National Chung Cheng University.

<sup>5</sup>Research Center for Environmental Changes, Academia Sinica.

Corresponding author: Hao Kuo-Chen ([kuochenhao@ntu.edu.tw](mailto:kuochenhao@ntu.edu.tw))

## Key Points:

- An optimized local 1D velocity model was determined from the regional seismic network.
- A subduction-to-strike-slip transition system could result in the near-vertical dip-slip tear slab in the southeastern Solomon Islands.
- The “jelly sandwich” rheology of the continental crust of the Australia Plate is observed.

## 21 **Abstract**

22 The Solomon Islands is one of the most seismically active areas in the southern Pacific with  
23 high earthquake hazard potential. The regional seismic network, equipped with six broadband  
24 seismic stations, was constructed as late as October 2018. On January 27 and 29, 2020, two  
25 moderate earthquakes, Mw 6.3 and 6.0, respectively, occurred in the southeastern Solomon  
26 Islands. The entire foreshock-main-shock-aftershock sequence was recorded by this seismic  
27 network for exploring the seismogenic structures. Based on the spacial distribution of the  
28 foreshock-aftershock sequence, the interaction of the subduction and transform zones between the  
29 Pacific and the Australia plates could lead to the near-vertical dip-slip tear slab. Confirmed with  
30 PREM and the new 1D velocity model for testing the robustness of the earthquake locations, a  
31 seismic gap at depths from 25 to 35 km is observed as the “jelly sandwich” rheology of the  
32 continental crust of the Australia plate.

33

## 34 **Plain Language Summary**

35 To establish a seismic network is always the first step and essential for studying any  
36 researches related to earthquakes, especially in the Solomon Islands, one of the most seismically  
37 active areas in the southern Pacific. However, as late as October 2018, the regional seismic network  
38 in the southeastern Solomon Islands, equipped with six broadband seismic stations, was  
39 constructed because most of the areas are inaccessible. A good 1D local velocity model is crucial  
40 for determining earthquake locations. The data set from foreshock-main-shock-aftershock  
41 sequence of two earthquakes in 2020 recorded in the seismic network provides a good opportunity  
42 for obtaining a 1D velocity model. After the reliable earthquake locations are determined, the  
43 spacial distribution of the foreshock-aftershock sequence can provide valuable information about  
44 seismogenic structures for better understanding the occurrence of earthquakes. As a result, a near-  
45 vertical dip-slip slab of the Australia plate from the subsurface to 120 km with a seismic gap at  
46 depths from 25 to 35 km is observed for the first time. This near-vertical tear slab could result from  
47 a subduction-to-strike-slip transition system and the seismic gap within the continental crust is  
48 related to “jelly sandwich” rheology.

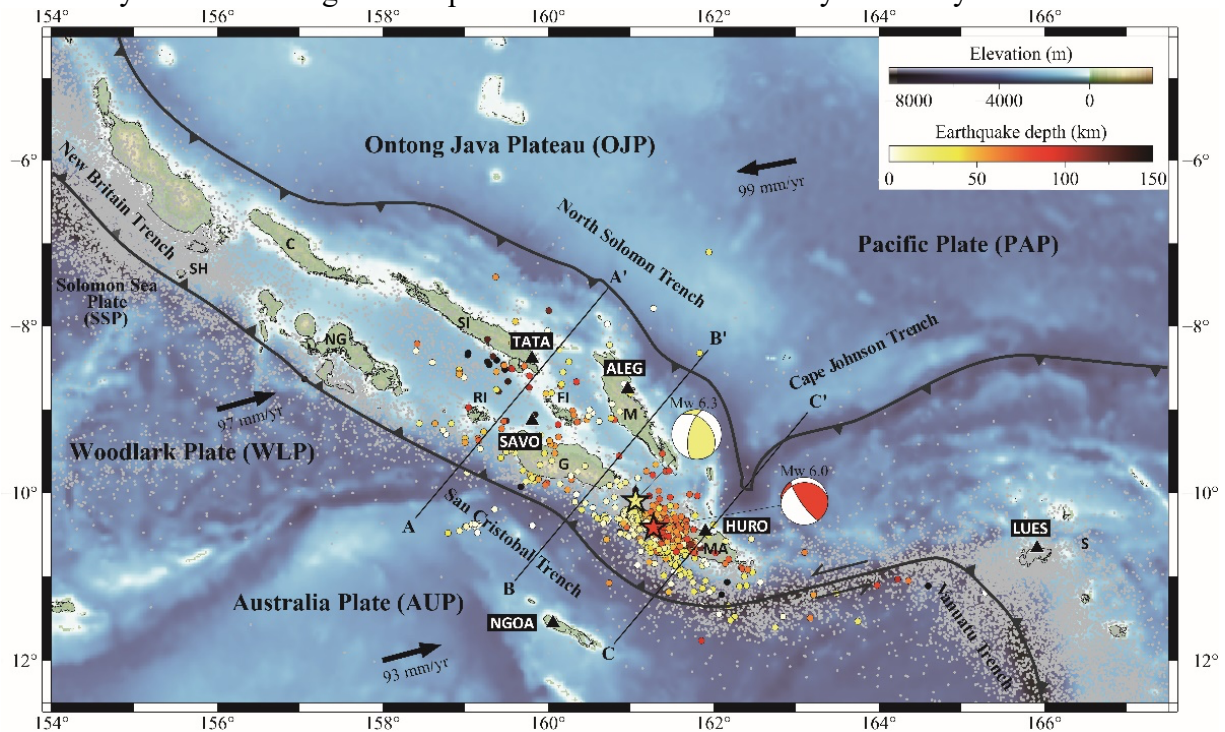
49

## 50 **1 Introduction**

51 Previous studies in the Solomon Islands have mainly focused on tectonic evolution (e.g., Yan  
52 and Kroenke, 1993; Mann et al., 1998; Petterson et al., 1999; Mann and Taira, 2004; Holm et al.,  
53 2016), geology (e.g., Mann et al., 1998; Taylor et al., 2005; Taylor et al., 2008; Chen et al., 2011),  
54 and a few related to the crustal and upper mantle structures using ocean-bottom seismometer data  
55 set with passive and active sources (e.g., Mann et al., 1996; Phinney et al., 1999; Mann and Taira,  
56 2004; Miura et al., 2004). The subduction systems in the southeastern Solomon Islands have not  
57 been documented in detail due to shortages of seismic stations and feasible data for investigating  
58 the complex seismogenic, crustal, and upper mantle structures. The complex tectonic setting and  
59 geopolitical marginality make the Solomon Islands hardly to be explored, including deploying  
60 seismic stations on islets. However, improvement of station coverage, in particular, is one of the  
61 most effective observations to answer the seismotectonic debate (e.g., Ku et al., 2020).

62 The regional seismic monitoring network in the southeastern Solomon Islands was  
63 constructed until October 2018 (Fig. 1). On January 27 and 29, 2020, two moderate

64 earthquakes, Mw 6.3 and Mw 6.0, respectively, occurred in the southeastern Solomon Islands. The  
 65 entire foreshock-main-shock-aftershock sequences were completely recorded by this regional-  
 66 scale seismic network. These two earthquakes are located in the most active area of the region,  
 67 which the foreshock and aftershock sequences can provide a unique opportunity to look into the  
 68 crustal and upper mantle structures of the subduction zones between the Pacific plate (PAP) and  
 69 the Australia plate (AUP). Here, we report on earthquake distribution for the southeastern  
 70 termination of the southeastern Solomon Islands subduction zone and also derive a optimized local  
 71 1D velocity model utilizing the complete seismic data recorded by the newly seismic network.



72  
 73 **Figure 1.** Topography, bathymetry, and regional tectonic setting of the Solomon Islands region.  
 74 Arrows indicate direction and rate of plate motion of the Australia, Pacific, and Woodlark plates  
 75 (NUVEL-1A, Demets et al., 1994); heavy lines with triangles represent subduction boundaries;  
 76 black triangles are broadband seismic stations; yellow and orange stars represent earthquakes  
 77 occurred on January 27 and 29 from the Incorporated Research Institutions for Seismology (IRIS)  
 78 catalog; focal mechanisms of the two earthquakes are from GCMT; circles color-coded by depth  
 79 indicate foreshocks and aftershocks recorded by GNS seismic stations; background seismicity are  
 80 shown as gray dots and are compiled by the IRIS event catalog for the period 1971-2021; AA',  
 81 BB' and CC' are the cross sections in Figs. 2-5. SH, Shortland Islands; C, Choiseul; NG, New  
 82 Georgia Island Group; SI, Santa Isabel; RI, Russell Islands; FI, Florida Islands; G, Guadalcanal;  
 83 M, Malaita; MA, Makira; SCZ, Santa Cruz Islands.

## 85 2 Tectonic setting

86 The Solomon Islands is located in a complex and active plate boundary where several  
 87 plates interact with each other, including the PAP, the AUP, and the associated microplates (i.e.,  
 88 the Woodlark plate (WLP) and Solomon Sea plate (SSP)) (Fig. 1) (e.g., Demets et al., 1990, 1994,  
 89 2010; Beavan et al., 2002; Miura et al., 2004; Phinney et al., 2004; Taira et al., 2004; Taylor et al.,  
 90 2005, 2008; Argus et al., 2011; Newman et al., 2011). In the southern Solomon Islands, the WLP  
 91 and the AUP subduct beneath the PAP forming the New Britain Trench, San Cristobal Trench and

92 Vanuatu Trench (e.g., Taylor and Exon, 1987; Crook and Taylor, 1994; Taylor et al., 1995; Mann  
93 et al., 1998; Taylor et al., 2005). The area surrounding the Solomon Islands and the Santa Cruz  
94 Islands contains two subduction-to-strike-slip transition (SSST) regions where a transform zone  
95 links two oblique subduction zones (Bilich et al., 2001). In addition, the Ontong Java Plateau of  
96 the PAP, the largest and thickest oceanic plateau on Earth, subducts along the North Solomon  
97 Trench and the Cape Johnson Trench in the north with slight convergence (e.g., Taylor and Exon,  
98 1987; Yan and Kroenke, 1993; Crook and Taylor, 1994; Mann et al., 1998; Petterson et al., 1999;  
99 Mann and Taira, 2004). The Solomon arc is assumed the most representative example of an island  
100 arc polarity reversal due to the presence of inwardly double subduction zones resulting in high risk  
101 of earthquakes, tsunamis, and volcanic eruptions.

102 Composed of two chains of islands, the Solomon Islands extends about 1000 km wide  
103 which are partitioned into multiple segments by distinct geological or seismological characteristics  
104 (e.g., Mann et al., 1998; Taylor et al., 2005; Chen et al., 2011). Nowadays, the active subduction  
105 occurs in the southeast of the Solomon Islands along the San Cristobal Trench according to  
106 previous seismological investigations from global seismic networks (e.g., Cooper and Taylor,  
107 1987; Mann et al., 1998; Chen et al., 2011). They found that it might be caused by strongly oblique  
108 subduction occurring southeast of the region, although the structures of subduction zones is still  
109 under debate.

110

### 111 **3 Seismic network and data processing**

112 The Institute of Geological and Nuclear Sciences Limited (GNS), New Zealand, deployed six  
113 permanent seismic stations in different islets of the southeastern Solomon Islands since October  
114 2018 (Fig. 1). The instruments are equipped with broadband seismometer (Trillium 120PA;  
115 Nanometrics Inc., Canada) and 24-bits digital recorder (Q330S; Quanterra Inc., U.S.A.) with  
116 sampling rates of 100 Hz. Except for the timing problem of the station LUES, most of the seismic  
117 waveforms recorded by the other five stations have good signal-to-noise ratios. To date, this  
118 seismic network is maintained by the Ministry of Mines, Energy and Rural Electrification of the  
119 Solomon Islands Government.

120 In this study, we processed two-month continuous seismic waveforms from this seismic  
121 network, one month before and after the two main shocks, respectively, to well cover the period  
122 of the whole earthquake sequence. The data set is formatted with the daily miniSEED and we used  
123 the SeisAn Earthquake analysis software (SEISAN) to establish the event database (Havskov and  
124 Ottemoller, 1999). Most of the events occurred close to the seismic network so that we were able  
125 to extract numerous high-quality seismic waveforms to pick P- and S-wave arrivals, locate  
126 earthquakes and determine magnitudes. We located earthquakes by the HYPOCENTER program  
127 (e.g., Lienert et al., 1986) and determined moment magnitude ( $M_w$ ) by spectral analysis. More  
128 details of the waveform analysis procedure are described in Havskov and Ottemoller (2010).

129 The earthquake catalog contains events detected by at least three stations and has more than  
130 one clear S-wave arrival to effectively constrain the depths of earthquakes. The interpolated 1D  
131 Preliminary Reference Earth Model (PREM) (Dziewonski and Anderson, 1981) was used as the  
132 reference model. In total, 730 earthquakes were listed in the preliminary catalog and of which 651  
133 were located within the seismic network. We used the program VELEST (Kissling, 1988, Kissling  
134 et al., 1994) to derive a 1D velocity model, which produces the smallest possible uniform error for  
135 a set of seismic events with well-constrained locations. We select events within the range of the  
136 seismic network with the root-mean-square error in arrival time from 0.5 to 1.0 s to invert a new

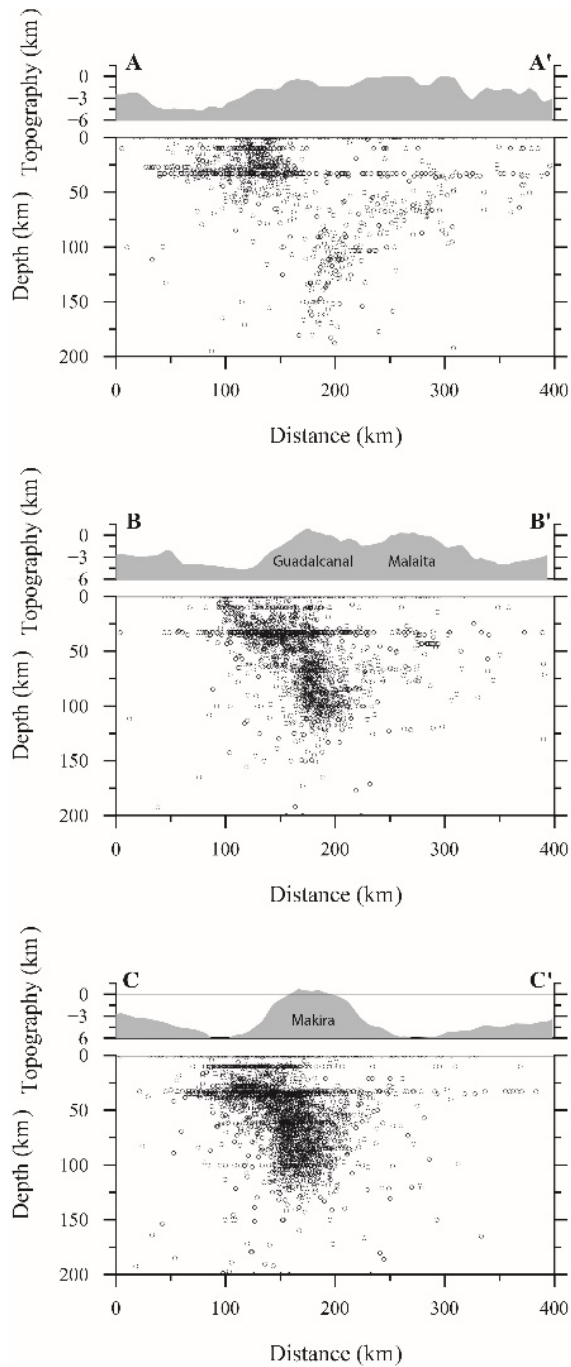
137 1D velocity model. In total, 389 events were selected for inversion to derive the preferred 1D  
138 model and then with it we relocated all 730 earthquakes to obtain the final catalog.

139

#### 140 **4 Results**

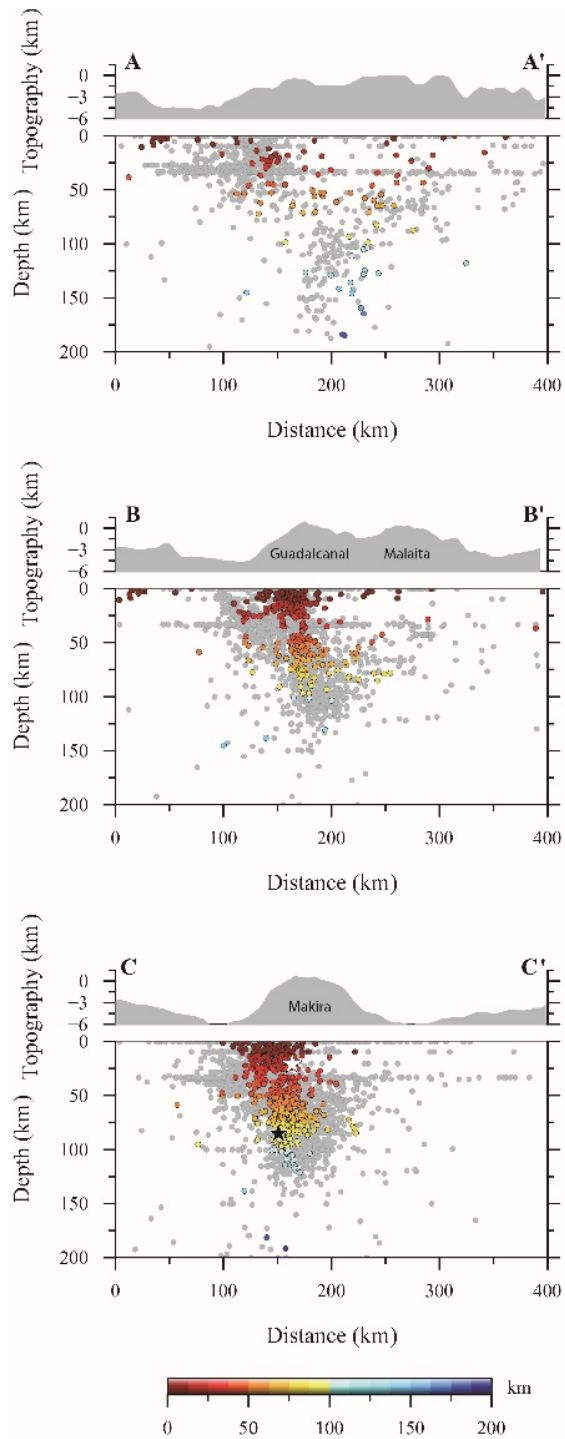
141 The background seismicity is extracted from the global earthquake catalog from 1971-2021  
142 compiled by the Incorporated Research Institutions for Seismology (IRIS) (Fig. 2). In 50 years,  
143 only ~5100 events in our study area are listed in the IRIS catalog because of poor constraints of  
144 station coverage. The hypocenters of the two main shocks, reported by IRIS, distribute apart from  
145 depths at 21 and 85 km, respectively (cross-section CC' of Fig. 3). During the same time period,  
146 January and February 2020, only 23 earthquakes are listed in the IRIS catalog but 730 are detected  
147 from our new data set. Obviously, we detected a significant number of missing events, especially  
148 at shallow depths that also appear with steep dip, the same as the deeper events (cross-sections  
149 BB' and CC' of Fig. 3). Relatively, in contrast, our results at deep depth show a similarity of high  
150 dip angle with background seismicity but are more concentrated at the San Cristobal Trench (cross-  
151 sections BB' and CC' of Fig. 3).

152 Among the 730 events, the standard error of the means in vertical location (ERZ), in  
153 horizontal location (ERH), and root-mean-square error in arrival time of event locations are  $24.7$   
154  $\pm 19.15$  km,  $13.43 \pm 10.8$  km, and  $0.61 \pm 0.30$  s, respectively. The moment magnitudes ( $M_w$ )  
155 determined in this study mostly range from 2.0 to 4.0. The main earthquake cluster is located  
156 between Makira and Guadalcanal (Fig. 1), one of the most active regions in the Solomon Islands,  
157 where commonly experiences large earthquakes (Chen et al., 2011). Events in the cluster extend  
158 from subsurface to 120 km depth which is similar to the previous studies (Cooper and Taylor,  
159 1985; Mann and Taira, 2004). Three southwest-northeast cross sections nearly perpendicular to  
160 the subduction zone show spatial variation of foreshocks and aftershocks from northwest to  
161 southeast (Figs. 2 and 3). Two southeastern cross sections close to the main shocks reveal that the  
162 event cluster is near-vertical and can be divided into shallow ( $< 25$  km) and deep (35-120 km)  
163 parts (cross-sections BB' and CC' of Fig. 3). Although the North Solomon Trench contains fewer  
164 earthquakes, the cross sections in the northwest do show two trenches subduct inwardly (cross-  
165 sections AA' and BB' of Fig. 3). Fig. 4 presents the cross sections of the relocated earthquakes  
166 with the new 1D velocity model. Both the location results with PREM and the new 1D velocity  
167 model reveal a steep event cluster, but the new velocity model has low-velocity zone at 10 km  
168 depth and slower velocity layer within depths of 25-35 km comparing with PREM (Fig. 5).



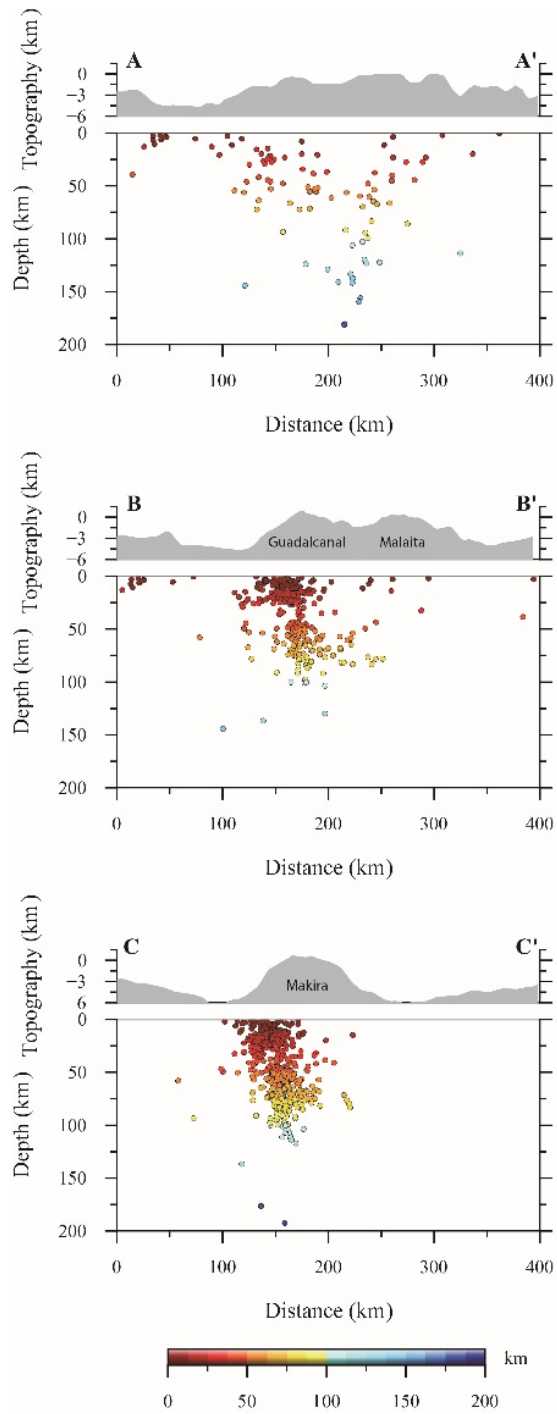
169  
170  
171  
172  
173

**Figure 2.** Cross sections of background seismicity around the southeastern Solomon Islands are compiled by IRIS event catalog from the period 1971-2021. Earthquake hypocenters are projected onto the three 200-km-wide transects shown in Fig. 1. Topography of three area is projected on to profiles in the upper panels.



174  
175  
176  
177  
178  
179

**Figure 3.** Comparison of earthquake hypocenters in this study and background seismicity. Cross sections with background seismicity (gray dots) and foreshocks and aftershocks (circles color-coded by depth); project lines are shown in Fig. 1; background seismicity is the same as Fig. 2; white and black stars represent January 27 and 29 earthquakes from IRIS event catalog.

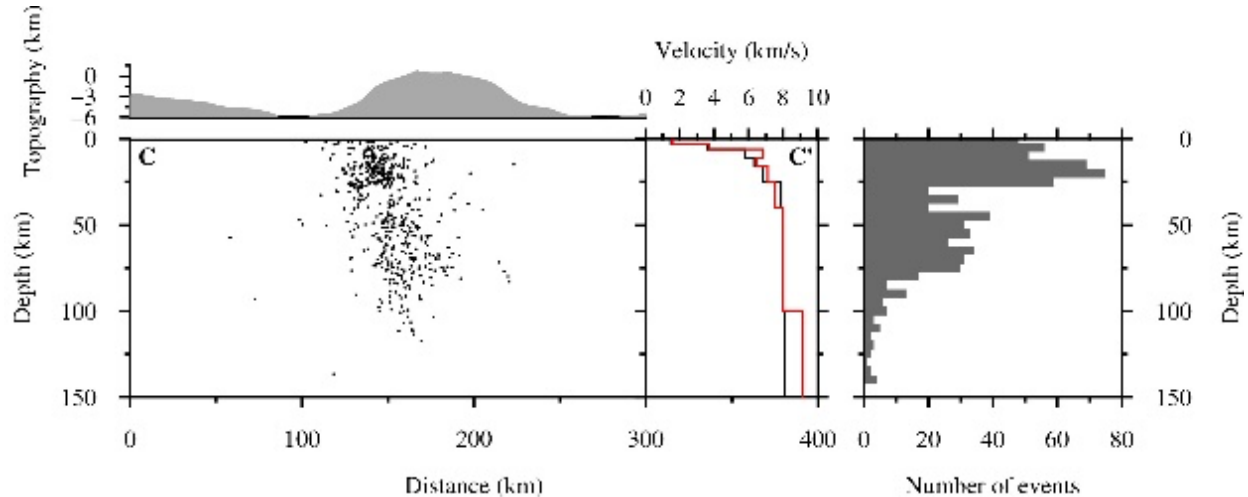


180

181

182

**Figure 4.** Cross sections of earthquake hypocenters relocated by the new 1D velocity model. Circles color-coded by depth are foreshocks and aftershocks; project lines are shown in Fig. 1.



183  
 184 **Figure 5.** CC' cross section (in Fig. 4) with the seismic cluster relocated by the new velocity model  
 185 around the southeastern Solomon Islands. The middle panel shows the 1D interpolated PREM  
 186 (black line) and the new velocity model (red line); the right panel is the event distribution in 5 km  
 187 depth intervals. Note the seismic gap between 25 km and 35 km depths.

188

## 189 5 Discussions

190 The Solomon arc, expanding ~1000 km wide, is characterized by diverse fault geometry as  
 191 well as subduction properties in different segments. The complexity of tectonic setting in the  
 192 Solomon Islands also makes the behavior of the seismic activities vary along the island chain. With  
 193 background seismicity from the 1971-2021 IRIS catalog in the Solomon Islands, majority of the  
 194 earthquakes occurred along the San Cristobal Trench which is much more seismically and  
 195 volcanically active than that of the early developed subduction zones to the north (Fig. 1). These  
 196 earthquakes, moreover, mainly distributed between Makira and Guadalcanal, show different  
 197 structural states from the northwestern side to the southeastern through the hypocenter transects  
 198 (Figs. 2 and 3). Many studies used seismicity from different global catalogs and time periods to  
 199 propose the subduction manifestation, including the dip angle and the depth of the two slabs from  
 200 the San Cristobal Trench and the North Solomon Trench (Cooper and Taylor, 1985; Mann and  
 201 Taira, 2004; Miura et al., 2004). Cooper and Taylor (1985) and Mann and Taira (2004) gave  
 202 different points of view from a similar distribution of seismicity between Makira and Guadalcanal  
 203 that the latter slab angle was much flatter than the former one. However, we have different  
 204 perspective of the subduction structure beneath the southeastern Solomon Islands from previous  
 205 studies due to the better quality constrains on the new seismic data set.

206 Based on our results, we suggest that the event cluster does show as a steep seismogenic  
 207 structure in the corner zone within the SSST between the Solomon Islands and the Santa Cruz  
 208 Islands and also could interpret it as the location of near-vertical dip-slip tear within the Australia  
 209 lithosphere (Fig. 5). This complicated plate configuration as a SSST region, which has been found  
 210 at least 30 locations on Earth (Bilich et al., 2001), is usually with damaged earthquakes occurred  
 211 frequently. The seismicity concentrates at the edge of the tear which extends almost vertically from  
 212 the subsurface to ~120 km. Govers and Wortel (2005) assumed that the intersection between the  
 213 subduction and the transform propagates through the lithosphere, inducing a tearing transform  
 214 fragment. They refer to the tearing as a subduction-transform edge propagator (STEP) fault and  
 215 developed the STEP model to interpret vertical, dip-slip tearing at perpendicular plate boundaries,

216 for example, the northern Tonga (Isacks et al., 1969; Millen and Hamburger, 1998) and the  
217 southeast corner of the Caribbean (Molnar and Sykes, 1969; Clark et al., 2008). According to  
218 Bilich et al. (2001), the southeastern Solomon Islands is one of the SSST regions where the  
219 northeastward subduction of the AUP connects the transition of northeast-southwest transform  
220 motion between the PAP and the AUP. We believe that the vertical motions and complex  
221 deformation revealed by the seismicity can demonstrate the tear propagation right beneath Makira  
222 and Guadalcanal. The suggestion is also consistent with Bilich et al. (2001) that the southeastern  
223 Solomon corner zone features a band of mechanisms which nearly reach the strike-slip corner (Fig.  
224 6).

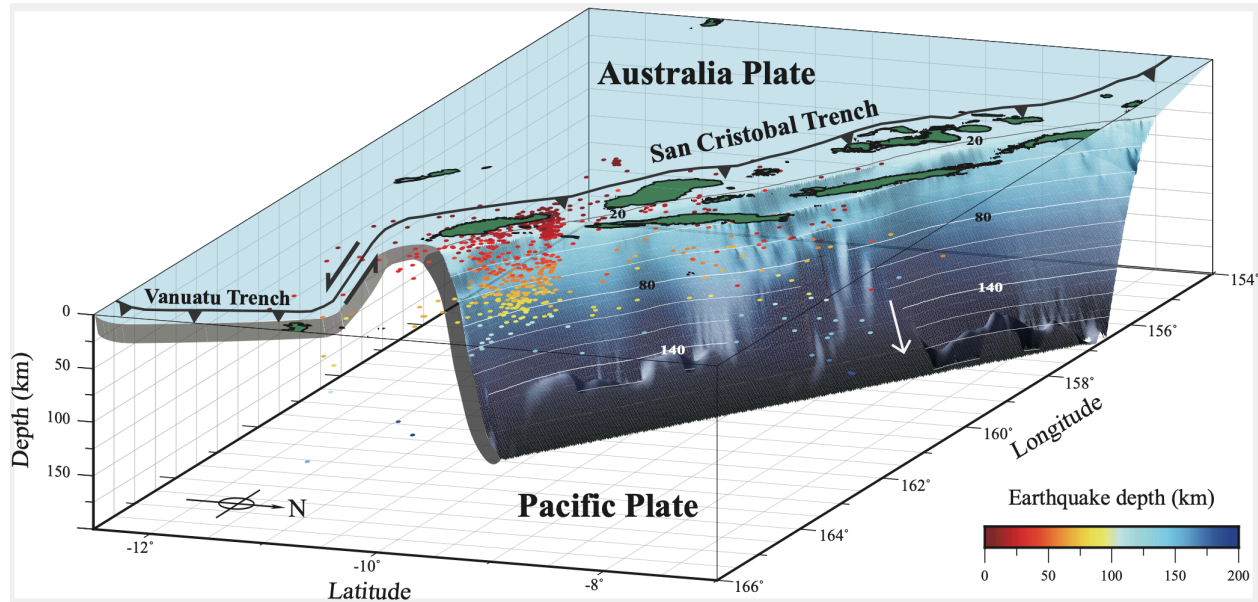
225 We also observe a seismic gap, both located by PREM (Fig. 3) and the new velocity model  
226 (Fig. 4), which is similar to the seismic cluster in the Lesser Antilles of the South American plate  
227 and this phenomenon is suggested that the gap is a weak, ductile, lower crustal layer separating a  
228 strong upper/middle crustal layer from a strong lithospheric layer (Clark et al., 2008). The seismic  
229 gap, known as the “jelly sandwich” rheology (Chen and Molnar, 1983; Watts and Burov, 2003),  
230 detaches the subducting and the buoyant pieces of the AUP along a near-vertical tear here. In  
231 comparison to significant strength in the dry upper mantle, the weak lower crust would show as  
232 the undried granulite in the continental lithosphere (Jackson, 2002). The whole seismogenic  
233 deformation is about 100 km wide and extends 120 km through the entire crust and lithosphere  
234 and the gap is at 25-35 km depth within the tear.

235 In order to derive the local 1D velocity model for earthquake location procedures, we use the  
236 program VELEST to construct the new velocity model in the southeastern Solomon Islands. In  
237 comparison with the interpolated PREM, the seismicity relocated by the new velocity model  
238 reveals that the earthquakes at shallow depth (~10 km) become deeper and the cluster also becomes  
239 more concentrated. Besides, a new optimized velocity model has a low-velocity layer around 10  
240 km depth and slower velocity from 20-35 km depth. Ku et al. (2020) also observed a low-velocity  
241 zone above the Moho in the Western Solomon Islands and they referred it to the lower crustal  
242 magma (Dufek and Bergantz, 2005). The distribution of the root-mean-square error in arrival times  
243 are more centralized after relocating and that may indicate the new optimized velocity model is  
244 more appropriate for this region. However, the cross sections in Fig. 4 show the appearance of  
245 earthquakes that relocated with the new velocity model is similar to Fig. 3, which events are located  
246 with the interpolated PREM. We can observe the seismic gap at depths of 20-35 km in both results  
247 which confirms the authenticity of the seismogenic structure.

248 Comparing the result with background seismicity, not only do we locate more earthquakes at  
249 shallow depth, but we also locate events more concentrated than the prior catalog (Fig. 3). We  
250 assume that nearby stations and the interpolated 1D PREM or the new velocity model constrain  
251 the quality of the result so that we can locate lots of earthquakes with small magnitude and at  
252 shallow depth. Owing to the complete seismic data recorded by the newly seismic network, we  
253 interpret the event cluster beneath Makira and Guadalcanal to define the location of active tearing  
254 within the Australia lithosphere, at the corner zone between the San Cristobal Trench and  
255 transform zone (Fig. 6).

256

257



258  
 259 **Figure 6.** Three-dimensional visualization of the seismic cluster in the southeastern Solomon  
 260 Islands viewed from northwest. Heavy lines with barbs represent subduction boundaries; solid  
 261 contour lines are Slab2 – A Comprehensive Subduction Zone Geometry Model (Hayes et al.,  
 262 2018), contoured every 20 km; earthquake hypocenters (circles) show crustal and mantle  
 263 seismicity gathers at 100 km-wide seismic cluster, at the edge of the lithospheric tear.

264

## 265 **6 Conclusions**

266 In this study, we provide better quality constraints on locating earthquakes with a new  
 267 optimized local 1D velocity model from the regional seismic network and discover the  
 268 seismogenic mechanisms and structures in the southeastern Solomon Islands. The earthquake  
 269 cluster between Makira and Guadalcanal distributes near vertically from subsurface to 120 km  
 270 depth, which is interpreted as the tear slab within the Australia lithosphere, due to the interaction  
 271 of subduction and transform zones of the PAP and AUP. A seismic gap observed at depths of 25-  
 272 35 km sustains a “jelly sandwich” rheology of the continental crust.

273

## 274 **Acknowledgments**

275 This project is supported by Academic Sinica (Grant NO. AS-TP-110-M02). The  
 276 assistance from Mr. Douglas Billy and Mr. Carlos Tatapu of Geological Survey Division, Solomon  
 277 Islands Ministry of Mines, Energy and Rural Electrification (MMERE) are highly appreciated.

278

## 279 **Open Research**

280 The seismic data set used in this manuscript is available on  
 281 <https://tecdc.earth.sinica.edu.tw/WAV/2020SolomonIs/> (login with Email:  
 282 solomon@earth.sinica.edu.tw and password: Islands2023).  
 283 Maps were created by using Generic Mapping Tools (GMT) version 6 (Wessel et al., 2019).

284

285

286 **References**

- 287 Argus, D. F., R. G. Gordon, and C. DeMets (2011). Geologically current motion of 56 plates  
288 relative to the no-net-rotation reference frame, *Geochemistry, Geophysics, Geosystems* **12**, no.  
289 11.
- 290 Beavan, J. P., M. Tregoning, M. Bevis, and C. Meertens (2002). Motion and rigidity of the Pacific  
291 plate and implications for plate boundary deformation, *J. Geophys. Res.* **107**, 2261.
- 292 Bilich A., C. Frohlich, and P. Mann (2001). Global seismicity characteristics of subduction-to-  
293 strike-slip transitions, *J. Geophys. Res.* **106**, no. B9, 19433-19452.
- 294 Chen M. C., C. Frohlich, F. W. Taylor, G. Burr, and A. Q. van Ufford (2011). Arc segmentation  
295 and seismicity in the Solomon Islands arc, SW Pacific, *Tectonophysics* **507**, 47-69.
- 296 Chen, W. P., and P. Molnar (1983). Focal depths of intracontinental and intraplate earthquakes  
297 and their implications of the thermal and mechanical properties of the lithosphere, *J. Geophys.*  
298 *Res.* **88**, no. B5, 4183-4214.
- 299 Clark, S. A., M. Sobiesiak, C. A. Zelt, M. B. Magnani, M. S. Miller, M. J. Bezada, and A. Levander  
300 (2008). Identification and tectonic implications of a tear in the South American plate at the  
301 southern end of the Lesser Antilles, *Geochemistry, Geophysics, Geosystems* **9**, no. 11.
- 302 Cooper, P. A., and B. Taylor (1985). Polarity reversal in the Solomon Islands arc, *Nature* **314**,  
303 428-430.
- 304 Cooper, P. A., and B. Taylor (1987). Seismotectonics of New Guinea: a model for arc reversal  
305 following arc-continent collision, *Tectonics* **6**, 53-67.
- 306 Crook, K., and B. Taylor, (1994). Structure and Quaternary tectonic history of the Woodlark triple  
307 junction region, Solomon Islands, *Marine Geophysical Researches* **16**, 65-89.
- 308 DeMets, C., R. G. Gordon, and D. F. Argus (2010). Geological current plate motions, *Geophys. J.*  
309 *Int.* **181**, 1-80.
- 310 DeMets, C., R. G. Gordon, D. F. Argus, and S. Stein (1990). Current plate motions, *Geophys. J.*  
311 *Int.* **101**, 425-478.
- 312 DeMets, C., R. G. Gordon, D. F. Argus, and S. Stein (1994). Effect of recent revisions to the  
313 geomagnetic reversal time scale on estimates of current plate motions, *Geophys. Res. Lett.* **21**,  
314 2191-2194.
- 315 Dufek, J., and G. W. Bergantz (2005). Lower crustal magma genesis and preservation: a stochastic  
316 framework for the evaluation of basalt-crust interaction. *J. Petrol.* **46**, 2167-2195.
- 317 Dziewonski, A. M., and D. L. Anderson (1981). Preliminary reference Earth model, *Physics of the*  
318 *Earth and Planetary Interiors* **25**(4), 297-356.
- 319 Forsyth, D. W. (1975). Fault plane solutions and tectonics of the South Atlantic and Scotia Sea, *J.*  
320 *Geophys. Res.* **80**, no. 11, 1429-1443.
- 321 Govers, R., and M. J. R. Wortell (2005). Lithosphere tearing at STEP faults: Response to edges  
322 of subduction zones, *Earth Planet. Sci. Lett.* **236**, 505-523.
- 323 Havskov, J., and L. Ottemoller (1999). SeisAn earthquake analysis software, *Seismol. Res. Lett.*  
324 **70**, no. 5, 532-534.
- 325 Havskov, J., and L. Ottemoller (2010). *Routine Data Processing in Earthquake Seismology*,  
326 Springer, Dordrecht, The Netherlands.
- 327 Hayes, G. P., G. L. Moore, D. E. Portner, M. Hearne, H. Flamme, M. Furtney, and G. M. Smoczyk  
328 (2018). Slab2, a comprehensive subduction zone geometry model, *Science* **362**, 58-61.
- 329 Holm, R. J., G. Rosenbaum, S. W. Richards (2016). Post 8 Ma reconstruction of Papua New

- 330 Guinea and Solomon Islands: Microplate tectonics in a convergent plate boundary setting,  
331 *Earth-Science Reviews* **156**, 66-81.
- 332 Isacks, B., L. R. Sykes, and J. Oliver (1969). Focal mechanisms of deep and shallow earthquakes  
333 in Tonga-Kermadec region and tectonics of island arcs, *Geol. Soc. Am. Bull.* **80**(8), 1443-1470.
- 334 Jackson, J. A. (2002). Strength of the continental lithosphere: time to abandon the jelly sandwich?,  
335 *GSA today* **12**, 4-10.
- 336 Kissling, E. (1988). Geotomography with local earthquake data, *Reviews of Geophysics.* **26**, no.  
337 4,659-698.
- 338 Kissling, E., W. L. Ellsworth, D. Eberhart-Phillips, and U. Kradolfer (1994). Initial reference  
339 model in local earthquake tomography, *J. Geophys. Res.* **99**, 19635-19646.
- 340 Ku, C. S., Y. T. Kuo, B. S. Huang, Y. G. Chen, and Y. M. Wu (2020). Seismic velocity structure  
341 beneath the Western Solomon Islands from the joint inversion of receiver functions and  
342 surface-wave dispersion curves, *Journal of Asian Earth Science* **195**, 104378.
- 343 Lienert, B. R. E., E. Berg, and L. N. Frazer (1986). Hypocenter: An earthquake location method  
344 using centered, scaled and adaptively least squares, *Bull. Seismol. Soc. Am.* **76**, 771-783.
- 345 Mann, P., and A. Taira (2004). Global tectonic significance of the Solomon Islands and Ontong  
346 Java Plateau convergent zone, *Tectonophysics* **389**, 137-190.
- 347 Mann, P., F. W. Taylor, M. B. Lague, A. Quarles, and G. Burr (1998). Accelerating late Quaternary  
348 uplift of the New Georgia Islands Group (Solomon Island arc) in response to subduction of  
349 the recently active Woodlark spreading center and Coleman seamount, *Tectonophysics* **295**,  
350 259-306
- 351 Mann, P., M. Coffin, T. Shipley, S. Cowley, E. Phinney, A. Teagan, K. Suyehiro, N. Takahashi,  
352 E. Araki, M. Shinohara, S. Miura, and L. Tivuru (1996). Researchers investigate fate of  
353 oceanic plateaus at subduction zones, *EOS Transactions American Geophysical Union* **77**,  
354 282-283.
- 355 Millen, D. W., and M. W. Hamburger (1998). Seismological evidence for tearing of the Pacific  
356 plate at the termination of the Tonga subduction zone, *Geology* **26**, no. 7, 659-662.
- 357 Miura S., K. Suyehiro, M. Shinohara, N. Takahashi, E. Araki, and A. Taira (2004). Seismological  
358 structure and implications of collision between the Ontong Java Plateau and Solomon Island  
359 Arc from ocean bottom seismometer-airgun data, *Tectonophysics* **389**, 191-220.
- 360 Molnar, P., and L. R. Sykes (1969). Tectonics of the Caribbean and Middle America region from  
361 focal mechanisms and seismicity, *Geol. Soc. Amer. Bull.* **80**, 1639.
- 362 Newman, A. V., L. J. Feng, H. M. Fritz, Z. M. Lifton, N. Kalligeris, and Y. Wei (2011). The  
363 energetic 2010  $M_w$  7.1 Solomon Islands tsunami earthquake, *Geophys. J. Int.* **186**, 775-781.
- 364 Petterson, M., T. Babbs, C. Neal, J. Mahoney, A. Saunders, R. Duncan, D. Tolia, R. Magu, C.  
365 Qopoto, H. Mahoa, and D. Natogga (1999). Geological-tectonic framework of Solomon  
366 Islands, SW Pacific: crustal accretion and growth within an intra-oceanic setting,  
367 *Tectonophysics* **301**, 35-60.
- 368 Phinney, E., P. Mann, M. Coffin, and T. Shipley (1999). Sequence stratigraphy, structure, and  
369 tectonics of the southwestern Ontong Java Plateau adjacent to the North Solomon trench and  
370 Solomon Islands arc, *J. Geophys. Res.* **104**, 20449-20466.
- 371 Phinney, E., P. Mann, M. Coffin, and T. Shipley (2004). Sequence stratigraphy, structural style,  
372 and age of deformation of the Malaita accretionary prism (Solomon arc-Ontong Java Plateau  
373 convergent zone), *Tectonophysics* **389**, 221-246.
- 374 Taira, A., P. Mann, and R. Rahardiawan (2004). Incipient subduction of the Ontong Java Plateau  
375 along the North Solomon trench, *Tectonophysics* **389**, 247-266.

- 376 Taylor, B., A. Goodliffe, F. Martinez, and R. Hey (1995). Continental rifting and initial sea-floor  
377 spreading in the Woodlark basin, *Nature* **374**, 534-537.
- 378 Taylor, B., and N. Exon (1987). An investigation of ridge subduction in the Woodlark – Solomons  
379 region: introduction and overview, in *Geology and Offshore Resources of the Pacific Island*  
380 *Arcs – Solomon Islands and Bougainville, Papua New Guinea regions* Taylor, B. (Editor),  
381 Circum-Pacific Council for Energy and Mineral Resources, vol. 7. Earth Science Series,  
382 Houston, TX, 1-24.
- 383 Taylor, F. W., P. Mann, M. G. Bevis, R. L. Edwards, H. Cheng, K. B. Cutler, S. C. Gray, G. S.  
384 Burr, J. W. Beck, D. A. Phillips, G. Cabioch, and J. Recy (2005). Rapid forearc uplift and  
385 subsidence caused by impinging bathymetric features: Examples from the New Hebrides and  
386 Solomon arcs, *Tectonics* **24**(6).
- 387 Taylor, F. W., R. W. Briggs, C. Frohlich, A. Brown, M. Hornbach, A. K. Papabatu, A. J. Meltzner,  
388 and D. Billy (2008). Rupture across arc segment and plate boundaries in the 1 April 2007  
389 Solomons earthquake, *Nature Geoscience* **1**, 253-257.
- 390 Watts, A. B., and E. B. Burov (2003). Lithospheric strength and its relationship to the elastic and  
391 seismogenic layer thickness, *Earth Planet. Sci. Lett.* **213**(1-2), 113-131.
- 392 Wessel, P., Luis, J. F., Uieda, L., Scharroo, R., Wobbe, F., Smith, W. H. F., & Tian, D. (2019).  
393 The Generic Mapping Tools version 6. *Geochemistry, Geophysics, Geosystems*, **20**, 5556–  
394 5564. <https://doi.org/10.1029/2019GC008515>.
- 395 Yan, C., and L. Kroenke (1993). A plate tectonic reconstruction of the SW Pacific, 0-100 Ma, in  
396 *Proceedings of the Ocean Drilling Program* Berger, T., Kroenke, L., Mayer, L., et al. (Editor),  
397 *Scientific Results* **130**, 697-709.
- 398
- 399